



Jet-BLR connection in the radio galaxy 3C 390.3

T. G. Arshakian¹, J. León-Tavares^{1,2}, A. P. Lobanov¹, V. H. Chavushyan², L. Popovic³, A. I. Shapovalova⁴, A. Burenkov⁴ and J. A. Zensus¹

¹ MPI für Radioastronomie, Auf dem Hügel 69, 53121 Bonn, Germany e-mail: tarshakian@mpi-fr-bonn.mpg.de

² Instituto Nacional de Astrofísica Óptica y Electrónica, Apartado Postal 51 y 216, 72000 Puebla, Pue, México

³ Astronomical Observatory, Volgina 7, 11160 Belgrade, Serbia

⁴ Special Astrophysical Observatory of the Russian AS, Nizhnij Arkhyz, Karachaevo-Cherkesia 369167, Russia

Abstract. Variations of the optical continuum emission in the radio galaxy 3C 390.3 are compared to the properties of radio emission from the compact, sub-parsec-scale jet in this object. We showed that *very long-term variations* of optical continuum emission (≥ 10 years) is correlated with the radio emission from the base of the jet located above the disk, while the optical *long-term variations* (1-2 years) follows the radio flares from the stationary component in the jet with time delay of about 1 year. This stationary feature is most likely to be a standing shock formed in the continuous relativistic flow seen at a distance of ~ 0.4 parsecs from the base of the jet. To account for the correlations observed we propose a model of the nuclear region of 3C 390.3 in which the beamed continuum emission from the jet and counterjet ionizes material in a subrelativistic outflow surrounding the jet. This results in the formation of two conical regions with double-peaked broad emission lines (in addition to the conventional broad line region around the central nucleus) at a distance ≈ 0.6 parsecs from the central engine.

Key words. galaxies: jets – galaxies: nuclei – galaxies: individual: 3C 390.3 – radiation mechanisms: non-thermal.

1. Introduction

Active galactic nuclei (AGN) are believed to be powered by accretion of a disk material into the central nucleus (or black hole; hereafter, BH). The accretion energy is transformed to the radiation of *thermal* variable continuum emission generated in the disk and to the kinetic energy of the bipolar outflows of plasma material ejected in the directions normal to plane

of the disk. In radio-loud AGN, the outflows (jets) are collimated and highly relativistic, and *synchrotron* continuum emission from jets may dominate at all energies (Ulrich et al. 1997; Worrall 2005). The continuum variable emission in these AGN may be related to both the jet and accretion flows and, hence, to be a mixture of thermal and non-thermal emission. It is believed that continuum radiation ionizes the clouds in the broad-line regions (BLR), therefore the localization of the source of variable

Send offprint requests to: T.G. Arshakian

continuum emission is instrumental for understanding the structure of the central engine and its operation. The jets originate very near to the BH and may trace the environment of an AGN from subpc- to kpc-scales in directions of advancing.

To localize the source of optical continuum emission in the jet we search for a positive correlation between the variability of the optical continuum flux and radio flux density of the parsec-scale jet for the radio-loud galaxy 3C 390.3 ($z = 0.0561$). We combined archived monitoring data of ≥ 100 optical data points with 10 radio points available from the very long baseline interferometry (VLBI) observations at 15 GHz made from 1992 to 2002 using the VLBA (Very Long Baseline Array). Although the radio sampling was poor we found a correlation at a confidence level of 90% between variations of the optical continuum and radio flux density of the stationary component (S1) of the jet (Arshakian et al. 2008). The potential source of optical emission was identified with S1 component - the VLBI core of the jet located at a distance of ≈ 0.4 pc from the central nucleus. Inspired by a relatively high significance of the correlation (while using only 10 radio points) and the link found between ejection epochs of jet components and maxima in the optical light curve, we propose a dense monitoring of six radio galaxies (including 3C 390.3) from 2005 using the VLBI and optical spectroscopy (with 2 meter class telescopes in Mexico) to check previous results.

2. Structure and kinematics of the VLBI jet

Modelfitting of a single epoch of VLBA image (Fig. 1) reveals five radio components on scales of 2 mas (1 mas = 1.09 pc). For 19 VLBA data sets from 1994 to 2008 we find two stationary components (S1 and S2) separated from D by 0.28 mas and 1.5 mas, respectively, and eight moving components (C4-C11). Apparent speeds of moving components lie between 0.8 c and 1.5 c . Back extrapolations of the fits to moving components allows the epochs of their ejection from D and epochs of

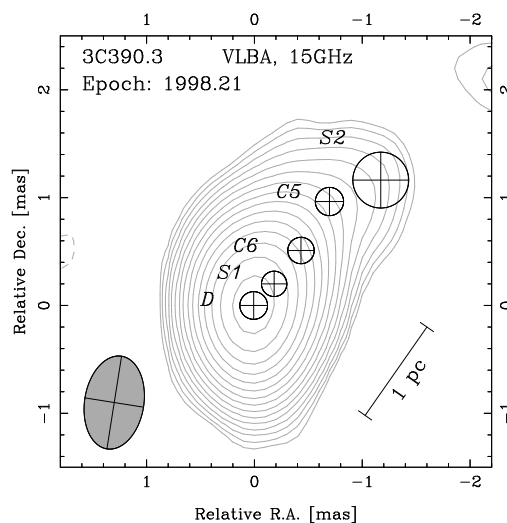


Fig. 1. A single epoch (1998.21) radio structure of 3C 390.3 observed with VLBA at 15 GHz.

passing through the stationary component S1 to be estimated (see bottom panel in Fig. 2). Variations of flux densities of two innermost stationary components (D and S1) of the jet are presented in Fig. 2 (panels (b) and (c)).

3. Couplings between subpc-scale jet and central engine

3.1. Jet - optical continuum

Variations of optical continuum fluxes at 5100 Å, H β emission line fluxes, flux densities from D and S1 stationary components of the jet at 15 GHz are shown in Fig. 2. Both radio (from D and S1) and optical variations have two independent components: long-term ($\lesssim 2$ yr) and very long-term ($\gtrsim 10$). This is evident also from the historical light curve of optical continuum in 3C 390.3 (see, for example, Shapovalova et al. 2001) which shows a superposition of short-term flares (few months), long-term (few years) and very long variations of tens years. Long-term flares from S1 component vary on timescales of $\lesssim 2$ yr, very similar to optical flares having comparable timescales (Fig. 2; panels (a) and (c)). Moreover, the relative amplitudes of optical and radio flares are comparable changing the intensity by a factor

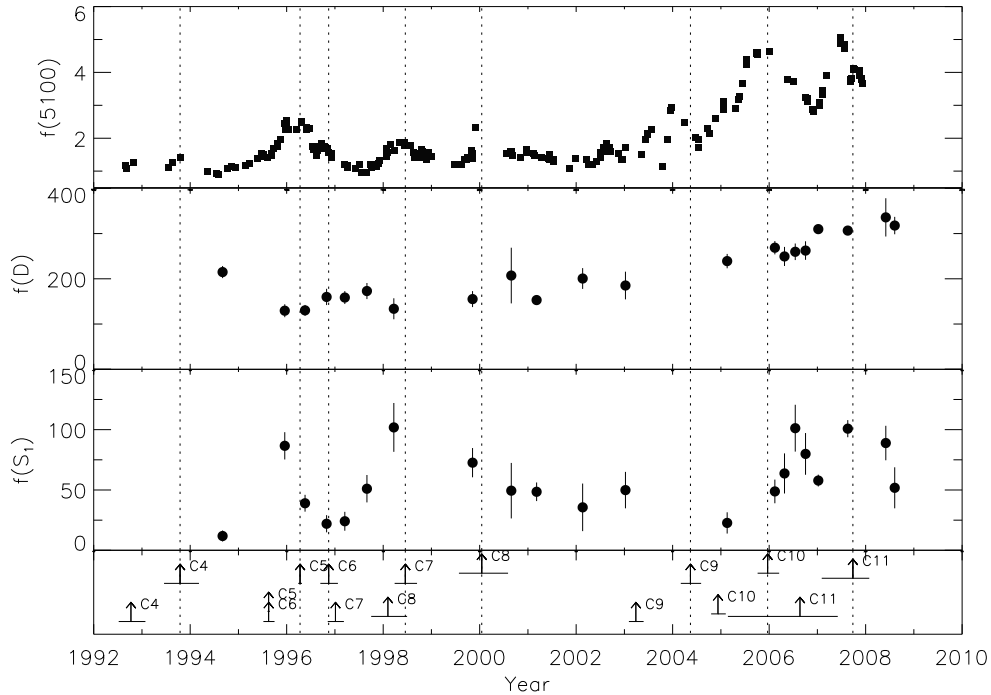


Fig. 2. The variations of the optical and radio fluxes of 3C 390.3 from 1992 to 2008 (Shapovalova et al. 2001; Sergeev et al. 2002, Shapovalova, priv. comm.; Tavares et al., in prep.). Optical continuum fluxes at 5100\AA (top panel; normalized to $10^{-15} \text{ erg s}^{-1} \text{ cm}^{-2} \text{ \AA}^{-1}$), radio flux densities from D and S1 stationary components of the jet at 15 GHz (panels (b) and (c)), and times of ejection of radio components at D (t_D ; grey triangles in the panel (d)) and times of passing the moving components through S1 (t_{S1} ; black triangles).

of 3 for optical continuum flux and factor of 4 in the case of radio flux from S1.

On the other hand, variations of radio emission from D is more smooth and follows the changes in the optical continuum on timescales of ≥ 10 yr (Fig. 2; panels (a) and (b)). To demonstrate the similarity of changes in optical and radio fluxes we fit the radio light curve and selected ranges in the minima of optical curve by polynomial function of the 4th order and presented the scaled fits in Fig. 3. The optical and radio (D) fluxes increase by the same factor (≈ 3 times) from 1996 to 2008 and have a surprisingly similar behavior. This suggests that optical variations on timescales of decades are related to radio variability of the component D, while optical long-term flares are cou-

pled with radio flares of S1 component of the jet.

Z-transformed correlation function (Alexander 1997) is used to calculate the correlation between $f(5100\text{\AA})$ and $f(S1)$ as this method can deal with sparsely sampled data. The distribution of time lags peaks around $1^{+0.06}_{-0.04}$ year with correlation coefficient of $0.54^{+0.26}_{-0.22}$. Although the uncertainties of the correlation coefficient are large (because of small radio sampling) there is an indication that the correlation could be real. This is evidenced by a similarity of the relative amplitudes and timescales of optical and radio (from S1) flares: optical and radio fluxes rise by a factor of ≈ 3 on timescales of 1.5-2 years. One could suggest that the radio emission from

S1 component leads the optical continuum emission with time lag of about one year.

We confirm the link between t_{S1} and maxima in the optical continuum flux (previously reported by Arshakian et al. 2008) for two new components, C9 and C10, ejected around 2004.3 (the C11 component is not taken into account because of large errors in t_{S1}). All seven ejection events occur within ~ 0.3 yr after a local maximum is reached in the intensity of the optical continuum. The probability that it happens by chance is very small (< 0.0001) suggesting that the process of passing of radio knots through S1 and reaching the maxima in the optical intensity are related.

3.2. Jet - BLR

The BLR in 3C 390.3 appears to be complex (Sergeev et al. 2002), probably because of multiple component structure of the emitting region. To check whether the $H\beta$ broad-line profile changes during long-term flares of the optical continuum emission, we averaged the $H\beta$ profiles during the minimum and maximum of the optical continuum (around 1994.5 and 1995 respectively). The averaged line profile in the minimum state has two peaks (red and blue) (Fig. 4; bottom solid profile), while in the maximum state it appears to have an additional central peak (Fig. 4; top solid profile) which is clearly seen also in the residual profile (dashed profile). The blue and red peaks are shifted at around -3000 km s $^{-1}$ and $+4200$ km s $^{-1}$, and central peak tends to be blueshifted around -350 km s $^{-1}$. This is a clear evidence that a new broad line region moving towards observer is excited during the maximum state of the optical flare.

4. Identification of D and S1 components

Identification of the regions D and S1 is important for understanding the structure of the central engine in 3C 390.3 and location of continuum sources producing the variable continuum radiation (Arshakian et al. 2008). If D would be the base of the counterjet we should expect that $f(D) < f(S1)$ because of

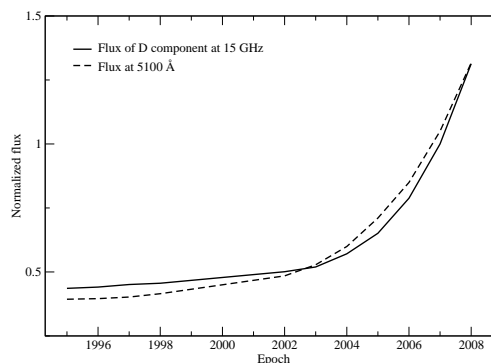


Fig. 3. Fits of normalized optical and radio (from D) light curves (dashed and solid lines respectively).

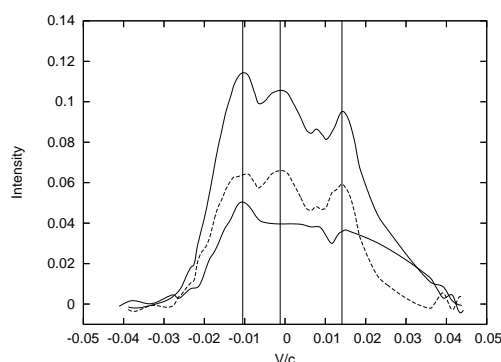


Fig. 4. The averaged $H\beta$ broad-line profiles in the maximum and minimum states of the optical continuum (top and bottom solid lines) and the residual profile (dashed line) between them.

relativistic (Doppler) deeming effect. The fact that $f(D) > f(S1)$ over 14 years of monitoring period rules out D being the base of the counterjet. It is likely that D is the base of the jet located near the BH. This idea is supported by the link between the ejection epochs of the components C5 and C8 from D and the dip in the X-ray flux and hardening of the spectrum (Arshakian & Belloni 2006), similar to radio galaxies 3C 120 and 3C 111 (Marscher et al. 2002; Marscher 2006). This correlation was interpreted as an accretion of the X-ray emitting gas in the disk into BH and ejection of a fraction of the infalling matter into the jet (Marscher et al. 2002). The base of the jet (or D component) is likely to be

located near the BH in or above a hot corona. The jet plasma material is then accelerated and collimated by helical magnetic fields and produces standing conical shock (Gómez et al. 1995) seen at radio wavelength at a distance of $\lesssim 1$ pc from the BH. Such a standing feature is seen in VLBI images of almost all radio-loud AGN and is known as the core of the jet. We associate the stationary component S1 (at a 0.3 pc projected distance from D) with the VLBI core of the jet.

5. Models of the central subpc-scale region

Here we discuss the results of previous sections and draw possible emission models of the central engine.

The conventional *source of thermal variable optical emission* is located in the disk and powered by the accretion of disk material onto the central BH. Optical radiation ionizes the central BLR (CBLR) rotating around the BH at a distance $\lesssim 1$ pc. However, in powerful radio galaxies a *synchrotron variable optical radiation* can be generated also in the relativistic jet. Depending on location of the source of optical continuum emission different regions of broad-line emission can be excited along the jet provided there is enough gas. According to present models of relativistic jets (Marscher et al. 2008, and references therein) the plasma material accreted onto central nucleus is accelerated and collimated by helical magnetic fields up to a distance of $\sim 10^4$ Schwarzschild radii. In this region the beamed X-ray, UV, optical and radio continuum emission can be generated. Due to synchrotron self absorption in the jet the beamed X-ray emission is radiated near the central nucleus, while UV and optical emission would appear with some time delay at larger distances, $\lesssim 1$ pc. The observed $H\beta$ emission line of the CBLR can be excited by both the beamed synchrotron optical emission of the jet and thermal optical emission from the disk. At the end of the acceleration and collimation zone the jet flow becomes turbulent (because of absence of helical magnetic fields) and ends in a standing conical

shock which is associated with the VLBI core (S1 component for 3C 390.3). Electrons accelerated to high energies in the shock region generate synchrotron emission from radio to optical bands as evidenced from multi-waveband polarization variability in the quasar PKS 0420-014 (D’Arcangelo et al. 2007). The variability of radio and optical emission from the jet core region can be understood in terms of disturbances in the jet (moving radio knots) originated near the central nucleus and spiraling along the jet streamline. Energy released from interaction of moving radio features with the standing shock generates the variable non-thermal radio and optical emission, which can ionize the gas in the rotating subrelativistic outflow (Murray et al. 1997; Proga et al. 2000) surrounding the jet and thus ionize the second outflowing BLR (OBLR) elongated along the jet. In BL Lac type objects (in which the jet oriented near the line of sight) moving components also may enhance the radio emission, optical, X-ray and even Gamma-ray emission when passing near the line of sight of the observer. In the case of 3C 390.3 the jet is inclined at $\approx 50^\circ$, hence, the Doppler beaming of optical emission from moving components should be weak but it may ionize the BLR and thus contribute to the flux of $H\beta$ emission line.

Variations of the $H\beta$ emission line follows the optical continuum flares with a time lag in the range between $\approx (20$ to $100)$ days (Dietrich et al. 1998; Shapovalova et al. 2001; Sergeev et al. 2002). An important question is in which BLR (CBLR or OBLR) the DP profile is generated. In 3C 390.3, the blue and red wings of the $H\beta$ emission line occur simultaneously (Shapovalova et al. 2001) implying that the DP emission lines should be generated in the same BLR, either in CBLR or OBLR. Moreover, the separation between blue and red peaks of the $H\beta$ emission line (Fig. 4) anticorrelates with intensity of optical continuum emission (Shapovalova et al. 2001).

5.1. The DP profile generated in the outflowing BLR

In the model where the non-thermal variable optical continuum emission of the jet ionizes

the DP emission line, the source of long-term optical continuum emission should be located at a distance of 0.3 pc from the radio core S1 (because of time lag of about one year between radio and optical flares), and at a distance of ~ 0.6 pc from the central BH. Such long-term optical flares can be produced by inverse Compton scattering of radio photons (from S1 region) by relativistic electrons of the jet. Optical flare can illuminate the outflowing conical BLR giving rise to the DP emission line profile. Depending on the orientation of the jet the approaching and rotating outflow should imprint a prominent signatures on the broad emission lines such as blue-shifted and single-peaked. The blueshifted central peak of the $H\beta$ profile (Fig. 4) is a signature of the outflowing BLR. Adopting an inclination angle of 50° of the jet (Arshakian et al. 2008) we estimate the outflow speed of the BLR to be around 500 km s^{-1} while the maximum rotation velocity is $\sim 2000 \text{ km s}^{-1}$. Very long-term changes of thermal optical continuum emission are generated in the accretion disk, and correlated with radio emission of D component located above the disk near the hot corona.

5.2. The DP profile generated in the central BLR

There are two basic ways for attempting to avoid the necessity of forming at least a fraction of broad-line emission at a large distance above the accretion disk. In these cases, the broad-line emission would be produced in a canonical BLR above the accretion disk, relaxing the need to have a relation between broad-line emission and the continuum emission from the jet. These two alternative scenarios are considered below in more detail. The first alternative is to assume that the long-term and very long-term variable optical continuum is produced in the vicinity of the central engine located in D, followed by variations in the radio regime, with some delay between the two. This scheme requires that the variable optical continuum is produced near the location of the component D, and the broad-line emission is generated in a CBLR above the accretion disk. The radio emission from D should

follow the optical continuum with some delay, which cannot be measured from the existing data. In the maxima of optical emission the jet contribution to the continuum becomes significant and manifests itself by ionizing a conical volume of CBLR and/or OBLR along the jet direction and producing the central SP component in the $H\beta$ emission line profile (Fig. 4). In this scenario, the correlation observed between the radio and optical continuum fluxes (Fig. 2), in which the radio emission leads the optical continuum emission, has to be ignored. While the relative sparsity of the radio measurements leaves a theoretical possibility for such a confusion, the existing data indicate that the probability of it to happen is less than 5%. Therefore, this scheme also can hardly be adopted at present.

5.3. A binary black hole

The second alternative is to reconsider the binary black hole scenario proposed for 3C 390.3 by Gaskell (1996) and discussed by Eracleous et al. (1997) and Shapovalova et al. (2001). In the second scenario, the double-peaked lines are formed in a binary black hole system in which each black hole has an independent BLR (Gaskell 1996). The binary black hole scenario cannot explain the correlated, simultaneous variability of the red and blue wings of the $H\beta$ line (Shapovalova et al. 2001). If the two black holes are located in D and S1, the total mass of the binary must exceed $\sim 5 \times 10^9 (P_{\text{obs}}/1000 \text{ yr}) M_\odot$. The observed radial velocity changes indicate a possible periodicity shorter than 100 yr (Shapovalova et al. 2001), pushing the total mass of the binary to $\sim 10^{11} M_\odot$. The trends observed in the radial velocities cannot be reconciled with the orbital motion in a binary black hole (Eracleous et al. 1997). Thus a binary system with two black holes located in D and S1 also has significant difficulties with explaining the observed properties of 3C 390.3. The possibility that the black hole associated with D has a companion with a much smaller orbital separation cannot be ruled out at present, but it would face the same difficulties as in the scenario in which the

variable optical continuum is generated in the vicinity of D.

6. Discussion and conclusions

The scheme proposed in the previous section, where the long-term variable optical continuum emission is generated in the jet and DP emission line are produced in the jet-excited BLR, explains the correlations observed between the radio, optical and X-ray light curves, and relates them to the evolution of the compact relativistic jet on scales of $\lesssim 0.5$ pc. It requires that at least a fraction of the broad-line emission in 3C 390.3 is excited by the non-thermal variable continuum emission from the jet. The large distance of the jet-excited OBLR from the central engine challenges the existing models in which the broad-line emission is localized exclusively around the disk or near the central engine (Peterson et al. 2002). The existence of the jet-excited OBLR in 3C 390.3 will question the assumption of virialized motion in the BLR (Kaspi et al. 2000) of all radio-loud AGN, galaxies and quasars, and, hence, the applicability of the reverberation mapping (Peterson et al. 2002) to estimate the black hole masses of radio-loud AGN. Time delays and profile widths measured during periods when the jet emission is dominant may not necessarily reflect the Keplerian motion in the disk, but rather trace the rotation and outward motion in an outflow. This can result in large errors in estimates of black hole masses made from monitoring of the broad-line emission. In the case of 3C 390.3, the black hole mass (2.1×10^9 solar masses, M_{\odot}) estimated effectively from the measurements near the maximum in the continuum light curve (Shapovalova et al. 2001) is significantly larger than the values ($3.5\text{--}4 \times 10^8 M_{\odot}$) reported in other works (Wandel et al. 1999; Kaspi et al. 2000). This difference is reconciled by considering the line width and the time delay between the optical continuum and line fluxes near the minimum of the continuum light curve, which yields $M_{\text{bh}} = 3.8 \times 10^8 M_{\odot}$. The possible existence of an outflow-like region in a number of radio-loud AGN should be taken into account

when estimates of the nuclear mass are made from the variability of broad emission lines.

We analysed the combined radio VLBI (15 GHz) and optical data of double-peaked radio-loud galaxy over the period from 1994 to 2008.

1. The structure of the parsec-scale jet is analysed using 19 epochs of radio VLBI data. Two stationary components (D and S1) and eight moving radio features were identified on scales of few parsecs. Apparent speeds of moving components are estimated to be in the range from $0.8c$ to $1.5c$. Radio flares of S1 component happens on timescales of 1-2 years (long-term), while a radio flux density of D component increases gradually during the time period of 16 years (very long-term).
2. Variations of optical continuum has two components, one changing on timescales of 1-2 years and one on time-scales of few decades, similar to radio flares of S1 and D stationary components of the jet. We found a striking similarity in the *very long-term* behavior of optical and radio (D) emission indicating that they are physically linked. Identification of D component with the base of the jet suggests that both very long-term optical and radio emission have a thermal origin and are generated in the disk and hot corona above the disk, respectively.

Cross-correlation analysis showed that *long-term* optical variations follow a radio flares from S1 component with time lag of ≈ 1 year. The correlation coefficient is 0.56 with large uncertainties resulting from the sparsely sampled radio data. Identification of S1 component as the radio core of the jet suggested that the source of long-term optical emission is located at a distance of 0.6 pc from the central BH, and at 0.3 pc from the VLBI core of the jet (S1 component). The link between component S1 and optical continuum is also supported by the correlation between the local maxima in the optical continuum light curve and the epochs at which the moving components of the jet pass the stationary radio feature S1.

3. A model proposed for the central sub-parsec scale region in 3C 390.3 may account for the observed radio-optical correlations. According to this model a slowly changing thermal optical continuum emission is generated in the disk while the relativistic jet flow generates flares of optical synchrotron radiation on time scales of 1-2 years and at a distance of ~ 0.6 pc from the central BH. The optical emission of the jet ionizes the rotating and outflowing BLR which produces the double-peaked profile of the $H\beta$ emission line.

A denser VLBI radio sampling covering a time period of several years is needed to confirm the correlation between the sub-parsec-scale jet and variable optical continuum and further to test the model suggested for the nuclear region of radio-loud galaxy 3C 390.3. To understand whether this correlation is common for other galaxies we started the coordinated long-term radio-optical observations of nearby radio-loud galaxies.

Acknowledgements. VHC is supported by CONACYT research grant 54480 (México). LCP is supported by Ministry of Science of Serbia (project 146002) and the Alexander von Humboldt foundation. JT acknowledges support from the CONACyT program for PhD studies, the International Max Planck Research School (IMPRS) for Radio and Infrared Astronomy at the Universities of Bonn and Cologne and the DAAD for a short-term scholarship in Germany. AIS acknowledges support from RFBR (grant 06-02-16843). The National Radio Astronomy Observatory is a facility of the National Science Foundation operated under cooperative agreement by Associated Universities, Inc.

References

- Alexander, T. 1997, *Astronomical Time Series*, 218, 163
- Arshakian T.G., Belloni T., 2006, VI Microquasar Workshop: Microquasars and Beyond, ed Belloni, T., PoS (MQW6), 29
- Arshakian, T. G., Lobanov, A. P., Chavushyan, V. H., Shapovalova, A. I., & Zensus, J. A. 2008, *Relativistic Astrophysics Legacy and Cosmology - Einstein's*, 189 (arXiv:astro-ph/0602016)
- D'Arcangelo, F. D., et al. 2007, *ApJ*, 659, L107
- Dietrich, M., et al. 1998, *ApJS*, 115, 185
- Eracleous M., Halpern J.P., Gilbert A.M., Newman J.A., Filippenko A.V., 1997, *ApJ*, 490, 216
- Gaskell C.M., 1996, *ApJ*, 464, L107
- Gómez J.L., Marti, J.M.A., Marscher A.P., Ibanez J.M.A., Marcaide J.M., 1995, *ApJL*, 449, L19
- Kaspi S. et al., 2000, *ApJ*, 533, 631
- Marscher A.P. et al., 2002, *Nature*, 417, 625
- Marscher A.P., 2006, VI Microquasar Workshop: Microquasars and Beyond, ed Belloni, T., PoS (MQW6), 25
- Marscher, A. P., et al. 2008, *Nature*, 452, 966
- Murray N., Chiang G., 1997, *ApJ*, 474, 91
- Peterson B.M., 2002, *Advanced Lectures on The Starburst-AGN Connection*, eds Aretxaga I., Kunth D. & Mújica R., Singapore World Scientific, 3
- Proga D., Stone J.M., Kallman, T.R., 2000, *ApJ*, 543, 686
- Sergeev S.G., Pronik V.I., Peterson B.M., Sergeeva E.A., Zheng W., 2002, *ApJ*, 576, 660
- Shapovalova I.A. et al., 2001, *A&A*, 376, 775
- Ulrich M., Maraschi L., Urry C.M. 1997, *ARAA*, 35, 445
- Wandel A., Peterson B.M., Malkan M.A., 1999, *ApJ*, 526, 579
- Worrall D.M., 2005, *Multiband Approach to AGN*, eds Lobanov, A.P. & Venturi, T. *Memorie della Societa Astronomica Italiana*, 76, 28